Molecular Phylogenetics and Evolution 177 (2022) 107622

Contents lists available at ScienceDirect

Molecular Phylogenetics and Evolution

journal homepage: www.elsevier.com/locate/ympev

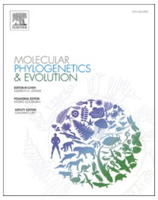

The evolutionary history of the relict scorpion family Iuridae of the eastern Mediterranean

Aristeidis Parmakelis [a,*], Domniki Dimitriadou [a], Evdokia Gkigkiza [a], Lydia Karampatsou [a], Iasmi Stathi [b], Victor Fet [c], Ersen A. Yağmur [d], František Kovařík [e]

[a] *Section of Ecology and Taxonomy, Department of Biology, National and Kapodistrian University of Athens, Greece*
[b] *Natural History Museum of Crete, University of Crete, Voutes University Campus, GR-70013 Heraklion, Crete, Greece*
[c] *Department of Biological Sciences, Marshall University, Huntington, WV 25755-2510, USA*
[d] *Celal Bayar University, Alaşehir Vocational School, TR-45600 Alaşehir, Manisa, Turkey*
[e] *P. O. Box 27, CZ-145 01, Praha 45, Czech Republic*

ARTICLE INFO

Keywords:
Ancient scorpion clades
Greece
Multi-locus phylogeny
Species delimitation
Turkey

ABSTRACT

Iuridae is a family of scorpions that exhibits a highly complex biogeographic and taxonomic history. Iuridae taxa are mainly found in Turkey and Greece, whereas a single species is found in northern Iraq. Several taxonomic revisions have been conducted on this family that initially comprised two genera. The latest taxonomic review, based on morphological and anatomical features, raised the number of Iuridae genera to four, and the number of species to 14.

Sequence data from three molecular markers (COX1, 16S rDNA, ITS1) originating from numerous Iuridae taxa were analyzed within a phylogenetic framework. Divergence time-estimate analyses, species delimitation approaches and estimation of ancestral areas were implemented in order to: (1) reconstruct the phylogenetic relationships of the Iuridae taxa, (2) evaluate the morphological classifications, and (3) obtain insights into the biogeographic history of the family in the East Mediterranean.

The multi-locus phylogeny clearly confirms an ancient division into two clades, Calchinae and Iurinae. Ancient patterns of isolation and dispersal are revealed. Both subfamilies are largely confined to the Anatolian peninsula and its few coastal islands; only the most derived genus *Iurus* has dispersed westward to Crete and Peloponnese. Based on our findings, three new genera of Iurinae (*Metaiurus, Anatoliurus*, and *Letoiurus*) are established. The genus *Neocalchas* emerges as one of the most ancient scorpion clades, with divergence time about 27 mya.

1. Introduction

The East Mediterranean scorpion family Iuridae is considered the most basally branching family in one of the major taxonomic divisions of the order, which is parvorder Iurida (Santibanez-Lopez et al., 2019a; Sharma et al., 2018; Sharma et al., 2015; Soleglad and Fet, 2003). Iuridae possess many relict morphological features. Their intriguing relationship with other scorpion families is a subject of an active current debate: a long-standing sister relationship (and a remarkable geographic disjunction) with the New World families Hadruridae and Caraboctonidae (Francke and Soleglad, 1980; Santibanez-Lopez et al., 2019b; Santibanez-Lopez et al., 2020; Soleglad and Fet, 2003) has been recently challenged in phylogenomic studies (Ballesteros et al., 2022; Santibáñez-López et al., 2022; Sharma et al., 2015).

The taxa of Iuridae (in a strict sense) are found predominantly in Turkey and Greece (including some Aegean islands) and are quite widespread (Fig. 1). However, until recently Iuridae were extremely rare in museum collections and any study of these interesting scorpions was severely limited. The first species of *Iurus* Thorell, 1876 was described from Greece (Peloponnese), a large and very conspicuous *I. dufoureius* (Brullé, 1832), which was also recorded for Crete; now Crete population is a separate species *I. dekanum* (Roewer, 1943). Another taxon from the middle Taurus Mountains of southern Anatolia was first described as a subspecies *Iurus dufoureius asiaticus* Birula, 1903. About the same time, a quite different scorpion genus *Calchas* Birula 1899, was described from northeastern Anatolia. *Calchas* remained obscure until the pioneering studies of Vachon (1971, 1974), who discovered its close relationship with *Iurus*. With additional material collected and analyzed (Francke

---

* Corresponding author.
E-mail address: aparmakel@biol.uoa.gr (A. Parmakelis).

https://doi.org/10.1016/j.ympev.2022.107622
Received 7 June 2022; Received in revised form 10 August 2022; Accepted 29 August 2022
Available online 2 September 2022

and Soleglad, 1980; Kinzelbach, 1975, 1980; Kritscher, 1993), a quite different story for Iuridae was revealed; it became clear that this family houses relict East Mediterranean taxa. The first pilot phylogeny of scorpions (Soleglad and Fet, 2003) established the basal position of Iuridae within non-buthid scorpions. One of the first DNA phylogenies generated by our research group (Parmakelis et al., 2006b) specifically addressed the intriguing genus *Iurus*.

Over the last decade, several taxonomic papers specifically devoted to Greek and Turkish Iuridae have been published (Fet et al., 2009; Kovařík et al., 2010; Soleglad et al., 2012; Stathi et al., 2010; Yağmur et al., 2015a, 2013, 2015b). These authors revised all known taxa of Iuridae in detail, discovered and studied many novel morphological traits, and described several new species and two new genera. A morphology-based phylogeny of Iuridae was established at species level, which, however, remained to be evaluated by DNA analysis. The cited taxonomic papers should be consulted for all details on species morphology and distribution. They include detailed labels and locality lists of hundreds of currently known museum specimens, most of which were collected recently by our research team and collaborators. Presently, the family Iuridae is comprised of four genera and 14 species.

In the present study, the phylogeny of the Iuridae family is reconstructed within a multi-locus molecular phylogeny framework. To the best of our knowledge, this is the first comprehensive phylogenetic study of Iuridae involving 12 out of the 14 Iuridae species currently known. In

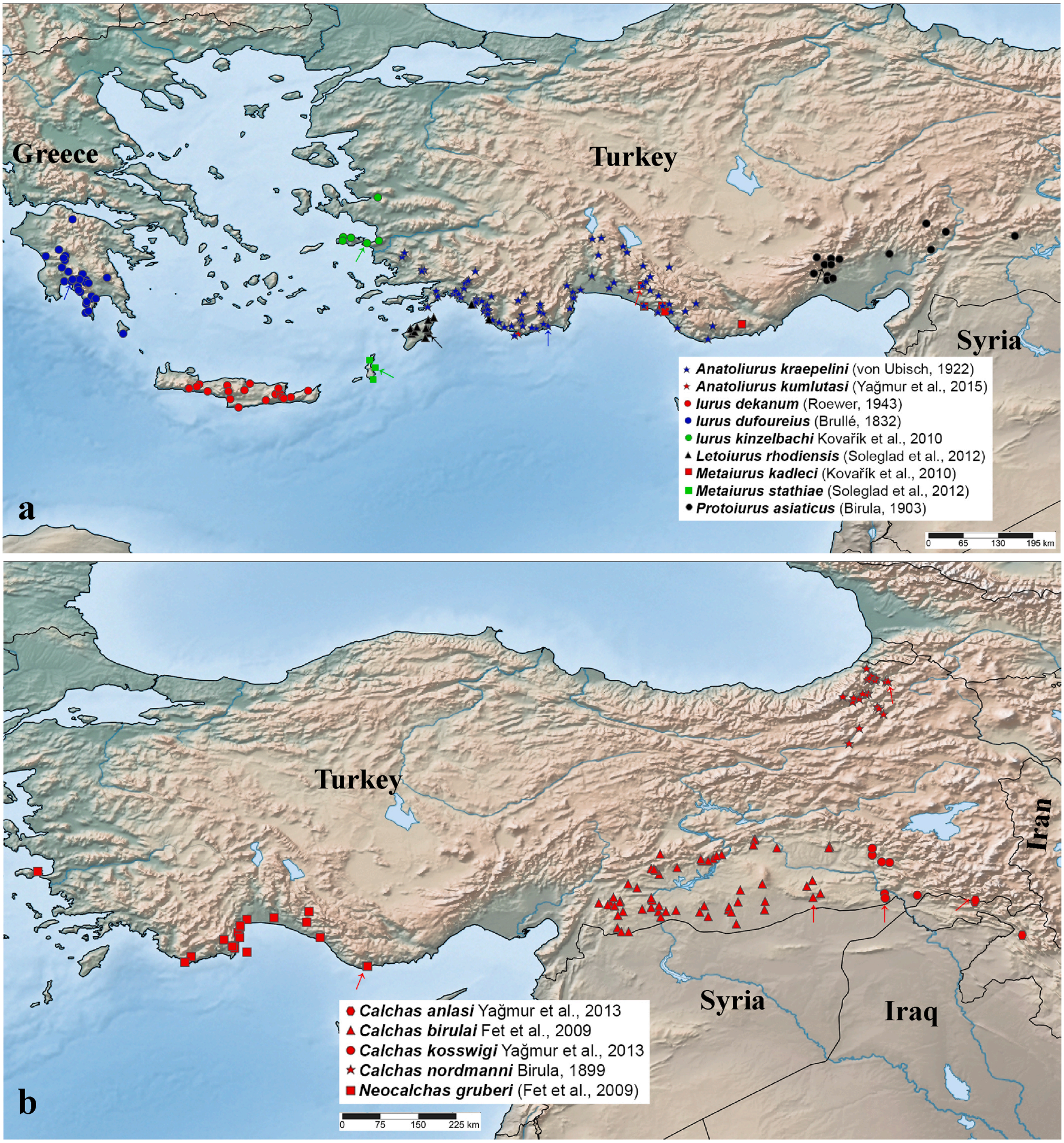

Fig. 1. **(a)** Distribution map of the subfamily Iurinae. **(b)** Distribution map of the subfamily Calchinae. In both maps, arrows next to species symbols indicate the type locality of the respective species. Maps were generated using SimpleMappr (Shorthouse, 2010).

addition, a molecular dating analysis was performed to reconstruct the evolutionary history of the family in the East Mediterranean.

2. Materials and methods

2.1. Samples, DNA extraction, amplification, and sequencing

In the present study, sequence data originating from 23 localities in Turkey and seven (7) localities in Greece (one mainland and six insular) are analyzed (Fig. 1). Details on the sequence data generated in the present study and those retrieved from GenBank are presented in Table 1. Geographic information relating to the sampled localities is provided in Table 1. The sampling within Turkey and Greece was quite extensive and covered the distributional range of all Iuridae species described from these areas (distributional ranges of taxa: Fig. 2). Specimens were assigned to species based on morphological characters (pedipalp chela morphology, trichobothrial patterns, etc.) following current taxonomy (Soleglad et al., 2012; Yağmur et al., 2013).

Genomic DNA was extracted from ethanol preserved specimens using either the CTAB protocol as modified by Parmakelis et al. (2003) or the NucleoSpin Tissue DNA purification kit (Macherey-Nagel), following the manufacturer's instructions. DNA extractions were visually inspected through electrophoresis in an ethidium bromide-stained agarose gel. DNA extractions and respective specimens are maintained in the laboratory of Dr. Parmakelis in the National and Kapodistrian University of Athens. For each specimen, through properly adjusted PCR assays, we aimed to amplify fragments of two mitochondrial DNA (mtDNA) and one nuclear DNA (nuDNA) marker. The mtDNA markers targeted were the cytochrome oxidase subunit I (COX1) and the large ribosomal subunit (LSU; 16S rDNA). The targeted contiguous nuclear region included the 3′ end of the small ribosomal subunit (SSU; 18S), the complete internal transcribed spacer 1 (ITS1), and the 5′ end of the 5.8S gene (henceforth called ITS1). In the amplification of the 16S rDNA, either the scorpion-specific primers reported by Gantenbein et al. (1999) or the universal primers (16S_BR_LR_12887/16S_AR_LR_13398) of Simon et al. (1994) were used. For the amplification of the COX1 gene fragment, the universal primers C1-N-2191 and C1-J-1718 (Simon et al., 1994) were used. The primer pair DT421/CS249 reported by Salomone et al. (2007) was used in the amplification of the ITS1 fragment. For each gene fragment, PCR reactions were performed in a 25-μL volume, where 1–2 uL of template DNA was mixed with 0.2 mM dNTPs, 0.25 uM of each primer, and 0.1 units of Taq Polymerase. The concentration of the $MgCl_2$ was 2.5 mM. Thermocycling was performed in either a MyCycler (Bio-Rad) or a TProfessional (Biometra) thermocycler. The cycle programs for 16S rDNA and COX1 comprised an initial denaturation step at 95 °C for 3 min, followed by 40 cycles of 30 s at 95 °C, 1 min at 40 °C, and 1.5 min at 72 °C. The cycling was ended with 10 min sequence extension at 72 °C. For ITS1, the PCR settings differed in the annealing temperature that was adjusted to 48 °C.

All PCR generated amplicons were purified using a commercial kit (Macherey-Nagel) before being sequenced. Automated sequencing of both strands of amplicons was performed using Big-Dye terminator chemistry. The primers used in the sequencing reactions were the same as in the PCR amplifications. At this point it must be noted that there were not any ITS1 sequences generated containing spurious ambiguous positions that would be indicative of heterozygous positions. All sequences produced for the present study have been deposited in GenBank. Accession numbers are provided in Table 1.

2.2. Alignment of sequences and analysis

Generated sequences were edited using CODONCODE ALIGNER, version 2.06 (Genecodes Corporation). The homology of the generated sequences to the targeted loci were evaluated through a BLAST search. In all alignment efforts CODONCODE ALIGNER and the Clustal algorithm was implemented. In all analyses, the gaps present in the alignments of the 16S rDNA and ITS1 were treated as missing. The genetic distances separating individual sequences were calculated using MEGA 7 (Kumar et al., 2016) and the uncorrected p-distance. This distance measure was estimated for each locus separately.

2.3. Phylogenetic analyses

Phylogenetic relationships were reconstructed using Bayesian Inference (BI) and Maximum Likelihood analysis (ML). Unless stated otherwise, PartitionFinder v.2.1.1 (Lanfear et al., 2016) and the Bayesian Information Criterion (BIC) were used to calculate and select the partitioning scheme and DNA substitution models that were the best fit for the dataset being analyzed. The phylogenetic methods described below were applied in three different datasets. The first dataset comprised only the COX1 and 16S rDNA sequence data, the second included only the nuclear region (ITS1), whereas the third dataset was concatenated comprising all three gene fragments. In all phylogenetic analyses we used *Hoffmannihadrurus aztecus* (Hadruridae) and *Euscorpius* cf. *corcyraeus* (Euscorpiidae) as outgroup taxa, whereas in the species delimitation approaches (see further below) only *Hoffmanihadrurus aztecus* was used as an outgroup. The sequence data of the outgroup species were retrieved from GenBank (see Table 1 for details). Details for the three different datasets and the partition scheme applied are given in Table S1. The phylogenetic trees were viewed with FigTree v.1.4.3.

Bayesian Inference was performed using MrBayes v.3.2.7 (Ronquist et al., 2012). The parameters of the different substitution models implemented, were unlinked across partitions. Two independent runs with four chains each were run for 10^7 generations. Parameters' sampling frequency was set to the default value. Evaluation of convergence between the different runs relied on the metrics suggested by the software's authors in the respective manual (Ronquist et al., 2020). More specifically, convergence of parameter values was assessed using TRACER, version 1.7.1 (Rambaut et al., 2018). Pooled postburn-in effective sample sizes (ESS) for all parameters were greater than 400, indicating that the pooled log file accurately represented the posterior distribution (Kuhner, 2009). In addition to the ESS values, for an analysis to be considered as having reached convergence, the average standard of split frequencies would have to be <0.01. The first 25% of the samples were discarded as burn-in. The remaining samples were used to summarize the parameters and the branch support (posterior probabilities, pp) of the inferred phylogenetic tree (50% majority rule consensus tree).

Maximum Likelihood was performed using the IQTREE2 software (Minh et al., 2020) through the web server https://iqtree.cibiv.univie.ac.at/. The partition scheme and the nucleotide substitution models applied in the dataset being analyzed was the one suggested by ModelFinder (Kalyaanamoorthy et al., 2017) as implemented in the model selection procedure of the IQTREE2 server. The partition of the dataset was provided as input but the "partition merging" option was selected, and the "relaxed clustering" value was set to 10% (partition merging was not implemented in the analysis of the dataset comprised only of ITS1). The consensus tree of the ML analyses relied on 10^3 bootstrap alignments using the ultrafast option of branch support analysis. In addition to the bootstrap branch support analyses, two additional branch support methods were also implemented in the ML phylogeny reconstruction. These were the SH-like approximate likelihood ratio test (Guindon et al., 2010) and the approximate Bayes test (Anisimova et al., 2011) as implemented in IQTREE2 software.

2.4. Species delimitation

Three different species delimitation methods were applied. The first one was the multi-rate Poisson Tree Processes (mPTP), which is an improved and more accurate method for delimiting species compared to the traditional PTP method (Kapli et al., 2017). The purpose of this analyses was to identify the "independently evolving" ingroup entities

Table 1

Details on the geographic origin of specimens/taxon used in the present work. Outgroup taxa are indicated. Sample codes of specimens as used in the phylogenetic analyses are given. GenBank accession numbers are provided. In the "Province" column "n.a." stands for Not Applicable.

Species	Country	Province	District	Locality	Latitude	Longitude	Sample code	GenBank Accession Numbers (16Sr DNA/COX1/ITS1)
Anatoliurus kraepelini	Greece	n.a.	South Aegean	Kastelorizo (Megisti) Island, Palaiokastro	36°08′20″	29°34′50″	S14_Kastelorizo	ON685236/ ON678023/ ON685282
Anatoliurus kraepelini	Greece	n.a.	South Aegean	Kastelorizo (Megisti) Island, Palaiokastro	36°08′20″	29°34′50″	S9_Kastelorizo	ON685233/ ON678020/ ON685279
Anatoliurus kraepelini	Turkey	Antalya	Akseki	Guzelsu Village, fork in the road	36°56′54.5″	31°45′41.7″	Gzs_50_1	ON685257/ ON678049/ ON685308
Anatoliurus kraepelini	Turkey	Antalya	Akseki	Guzelsu Village, fork in the road	36°56′54.5″	31°45′41.7″	Gzs_50_2	ON685258/ ON678050/ ON685309
Anatoliurus kraepelini	Turkey	Antalya	Alanya	Alanya	N/A	N/A	S16_Alanya	ON685237/ ON678024/ ON685283
Anatoliurus kraepelini	Turkey	Antalya	Elmali	Gomucu Village	36°24′04″	29°41′58″	Gmc_48_2	ON685255/ ON678047/ ON685306
Anatoliurus kraepelini	Turkey	Antalya	Elmali	Gomucu Village	36°24′04″	29°41′58″	Gmc_48_3	ON685253/ ON678045/ ON685304
Anatoliurus kraepelini	Turkey	Antalya	Finike	Alacadag Mountains, Turbe road	36°26′12″	30°02′22″	Roa_55_1	ON685261/ ON678053/ ON685312
Anatoliurus kraepelini	Turkey	Antalya	Goynuk	Goynuk Valley, Lycia road	36°41′18″	30°31′33″	Goy_49a_3	ON685256/ ON678048/ ON685307
Anatoliurus kraepelini	Turkey	Antalya	Kas	Elmali road	36°21′30″	29°29′00″	Elm_46_1	ON685250/ ON678042/ ON685301
Anatoliurus kraepelini	Turkey	Isparta	Eğirdir	Kovada Lake, fork in the road	37°38′01″	30°51′41″	Kov_53_1	ON685259/ ON678051/ ON685310
Anatoliurus kraepelini	Turkey	Konya	Beysehir	3 km SW from Kurucuova Village	37°40′27.1″	31°22′38.2″	Kur_54_1	ON685260/ ON678052/ ON685311
Calchas birulai	Turkey	Adiyaman	Gerger	Aydinlar Village	38°03′41″	39°06′44″	Ayd_4_1	ON685216/ ON678003/ ON685262
Calchas birulai	Turkey	Adiyaman	Gerger	Aydinlar Village	38°03′41″	39°06′44″	Ayd_4_3	ON685217/ ON678004/ ON685263
Calchas birulai	Turkey	Gaziantep	Araban	Köklüce Village	37°28′36″	37°36′51″	Kkl_14_1	ON685219/ ON678006/ ON685265
Calchas birulai	Turkey	Gaziantep	Araban	Köklüce Village	37°28′36″	37°36′51″	Kkl_14_2	ON685220/ ON678007/ ON685266
Calchas birulai	Turkey	Mardin	Mazıdağı	20 km W from Surgucu Village	37°30′02″	40°37′13″	Sur_17_1	ON685221/ ON678008/ ON685267
Calchas birulai	Turkey	Şanlıurfa	Siverek	Karacadağ Mts.	37°32′26″	39°49′55″	Kar_11_1	ON685218/ ON678005/ ON685264
Calchas kosswigi	Turkey	Siirt	Baykan	20 km SW from Baykan Town	38°03′08″	41°46′50″	Bay_20_1	ON685224/ ON678011/ ON685270
Calchas kosswigi	Turkey	Siirt	Central	2 km W from Meydandere Village	37°55′25″	42°05′14″	Mey_22_2	ON685225/ ON678012/ ON685271
Calchas kosswigi	Turkey	Siirt	Central	2 km W from Meydandere Village	37°55′25″	42°05′14″	Mey_26_3	ON685234/ ON678021/ ON685280
Calchas kosswigi	Turkey	Siirt	Central	2 km W from Meydandere Village	37°55′25″	42°05′14″	Mey_26_2	ON685232/ ON678019/ ON685278
Calchas nordmanni	Turkey	Artvin	Ardanuç	2 km W from Ardanuç Town, Cehennemderesi Valley	41°08′01″	42°03′01″	Ard_23_2	ON685226/ ON678013/ ON685272
Calchas nordmanni	Turkey	Artvin	Central	Hatila Valley NP, around entrance gate	41°13′01.5″	41°46′57.9″	Hat_24_2	

(*continued on next page*)

Table 1 (*continued*)

Species	Country	Province	District	Locality	Latitude	Longitude	Sample code	GenBank Accession Numbers (16Sr DNA/COX1/ITS1)
								ON685227/ ON678014/ ON685273
Calchas nordmanni	Turkey	Artvin	Central	Hatila Valley NP, around entrance gate	41°13′01.5″	41°46′57.9″	Hat_24_4	ON685228/ ON678015/ ON685274
Calchas nordmanni	Turkey	Artvin	Central	Hatila Valley NP, around entrance gate	41°13′01.5″	41°46′57.9″	Kar_11_2	ON685230/ ON678017/ ON685276
Calchas nordmanni	Turkey	Artvin	Yusufeli	Öğdem Village	40°54′49.2″	41°36′45.5″	Ogd_25_1	ON685229/ ON678016/ ON685275
Calchas nordmanni	Turkey	Artvin	Yusufeli	Öğdem Village	40°54′49.2″	41°36′45.5″	Ogd_25_4	ON685231/ ON678018/ ON685277
Iurus dekanum	Greece	n.a.	Crete	Rethymno, Mariou	35°12′03.0″	24°25′00.0″	I1_Crete	ON685238/ ON678027/ ON685286
Iurus dekanum	Greece	n.a.	Crete	Rethymno, Melisoudaki	35°16′30″	24°14′40″	S3_Crete	DQ106906/ ON678032/ ON685291
Iurus dufoureius	Greece	n.a.	Attiki	Kithira Island, Agia Sofia Cave	36°15′10″	22°59′40″	S1_Kithira	DQ106908/ ON678028/ ON685287
Iurus dufoureius	Greece	n.a.	Attiki	Kithira Island, Agia Sofia Ccave	36°15′10″	22°59′40″	S18_Kithira	ON685239/ ON678029/ ON685288
Iurus dufoureius	Greece	n.a.	Peloponnese	Messinia, Mani	36°45′40″	22°28′10″	S19_Peloponnisos	ON685240/ ON678030/ ON685289
Iurus dufoureius	Greece	n.a.	Peloponnese	Messinia, Mani	36°45′40″	22°28′10″	S20_Peloponnisos	ON685241/ ON678031/ ON685290
Iurus dufoureius	Greece	n.a.	Peloponnese	Messinia, Mani	36°45′40″	22°28′10″	S7_Peloponnisos	DQ106909/ ON678033/ ON685292
Iurus kinzelbachi	Turkey	Aydin	Kusadasi	Guzelcamli Village	37°41′22.15″	27°13′35.70″	Gzm_35a_1	ON685242/ ON678034/ ON685293
Iurus kinzelbachi	Turkey	Aydin	Kusadasi	Guzelcamli Village	37°41′22.15″	27°13′35.70″	Gzm_35a_2	ON685243/ ON678035/ ON685294
Metaiurus kadleci	Turkey	Antalya	Alanya	Tasatan Plateau	36°38′18.3″	32°03′35.1″	Tas_44_1	ON685248/ ON678040/ ON685299
Metaiurus stathiae	Greece	n.a.	South Aegean	Karpathos Island, Mesochori to Piles	35°30′ 55″	27°08′50″	S2_Karpathos	DQ106905/ ON678025/ ON685284
*Neocalchas gruber*i	Greece	n.a.	South Aegean	Kastelorizo (Megisti) Island, Palaiokastro	36°08′20″	29°34′50″	S10_Kastelorizo	ON685223/ ON678010/ ON685269
Neocalchas gruberi	Turkey	Antalya	Kas	between Kasaba and Kas Towns	36°14′47.7″	29°42′11.1″	Ksb_18_1	ON685222/ ON678009/ ON685268
Neocalchas gruberi	Turkey	Antalya	Kas	between Kasaba and Kas Towns	36°14′47.7″	29°42′11.1″	Ksb_18_2	ON685245/ ON678037/ ON685296
Protoiurus asiaticus	Turkey	Adana	Pozanti	Pozanti Town	37°26′09.7″	34°54′40.4″	Poz_42_1	ON685244/ ON678036/ ON685295
Protoiurus asiaticus	Turkey	Adana	Pozanti	Pozanti Town	37°26′09.7″	34°54′40.4″	Poz_42_2	ON685246/ ON678038/ ON685297
Protoiurus asiaticus	Turkey	Adana	Pozanti	Pozanti Town	37°26′09.7″	34°54′40.4″	Poz_42_3	ON685247/ ON678039/ ON685298
Letoiurus rhodiensis	Greece	n.a.	South Aegean	Rhodes Island, Masari	36°11′00″	28°04′40″	S12_Rhodes	ON685235/ ON678022/ ON685281
Letoiurus rhodiensis	Greece	n.a.	South Aegean	Rhodes Island, Masari	36°11′00″	28°04′40″	S8_Rhodes	DQ106907/ ON678026/ ON685285
Letoiurus rhodiensis	Turkey	Muğla	Fethiye	Domuz Island	36°39′58.1″	28°53′36.9″	Dom_45_1	

(*continued on next page*)

Table 1 (*continued*)

Species	Country	Province	District	Locality	Latitude	Longitude	Sample code	GenBank Accession Numbers (16Sr DNA/COX1/ITS1)
								ON685249/ ON678041/ ON685300
Letoiurus rhodiensis	Turkey	Muğla	Fethiye	Domuz Island	36°39′58.1″	28°53′36.9″	Dom_45_3	ON685252/ ON678044/ ON685303
Letoiurus rhodiensis	Turkey	Muğla	Fethiye	Faralya Village	36°29′41.1″	29° 8′15.0″	Far_47_1	ON685251/ ON678043/ ON685302
Letoiurus rhodiensis	Turkey	Muğla	Fethiye	Faralya Village	36°29′41.1″	29° 8′15.0″	Far_47_2	ON685254/ ON678046/ ON685305
	Outgroup taxa							
Euscorpius cf. *corcyraeus* (outgroup1)	Greece	n.a.	Epirus	Parga	39°16′58.9″	20°23′56.2″	*Euscorpius* cf. *corcyraeus*	KC215668/ KC215585/ KC215839
Hoffmannihadrurus aztecus (outgroup2)	Mexico			not specified	not specified	not specified	*Hoffmannihadrurus aztecus*	MF134787/ MF134686/not available

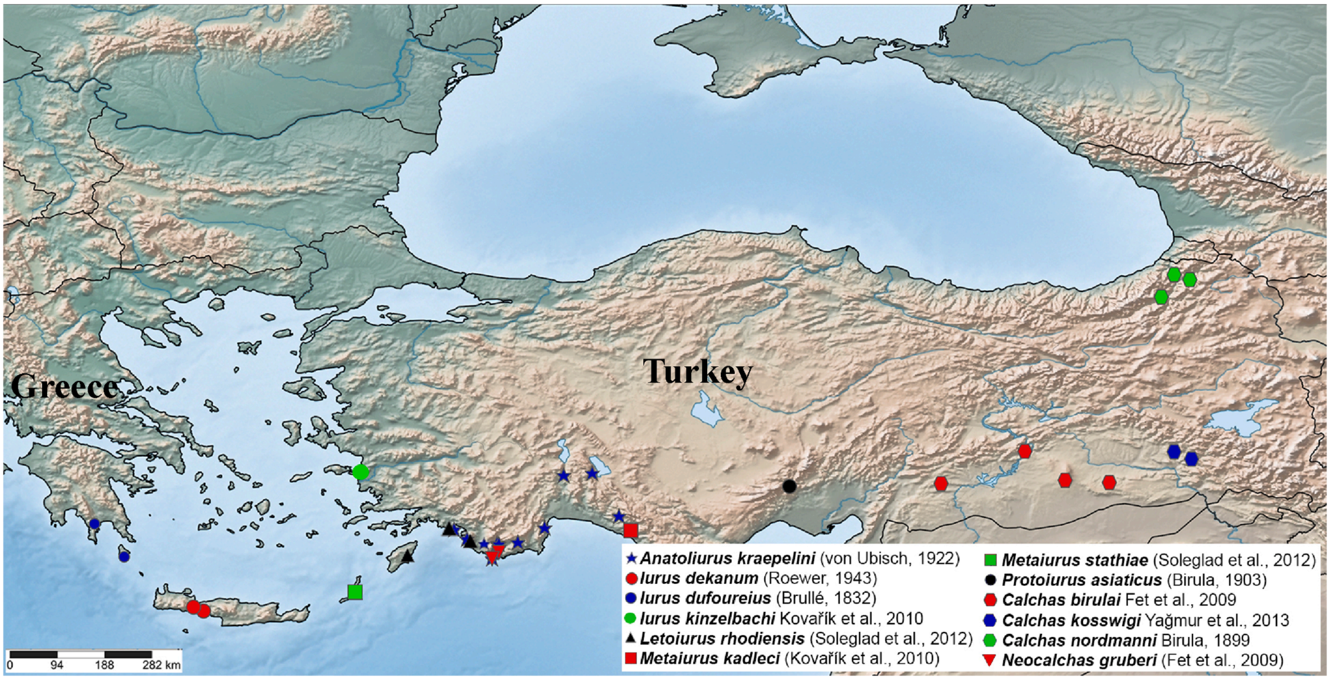

Fig. 2. Sampled Iurid specimens used in the analyses, originate from the localities depicted on the map. Geographic details of localities are provided in Table 1. The distributional ranges of the studied taxa are shown in Fig. 1.

based on the mtDNA gene fragments. Therefore, this analysis was applied only on the mtDNA dataset (see Table S1). The mPTP computes the ML delimitation from a phylogenetic tree provided as input and then, it computes the support values for each clade using MCMC, in order to assess the confidence of the ML delimitation (Kapli et al., 2017). The mPTP web server available at https://mptp.h-its.org/ was used to run the analysis. The input for the mPTP method was a binary, rooted Bayesian inference (BI) phylogenetic tree that was reconstructed with MrBayes v.3.2.7 using the settings described in the phylogenetic analyses above. For mPTP the Bayesian inference (BI) tree was rooted only with *Hoffmannihadrurus aztecus*.

The BEAST2 v.2.6.6 (Bouckaert et al., 2019) package STACEY v.1.2.5 (Species Tree And Classification Estimation, YARELY) was used to implement the second species delimitation method. STACEY implements a Bayesian method for inferring both species delimitations and species trees under the multispecies coalescent model using molecular sequences from multiple loci. For this method no a priori assignment of individuals and no guide tree are required (Jones, 2017). As stated in Jones (2017) when implementing STACEY, the minimal clusters may be merged but not split to form additional potential species. Since each minimal cluster holds one individual, the possible number of species ranges from one to the total number of individuals present in the analyses.

In the STACEY approach the concatenated dataset (Table S1) including both the mtDNA gene fragments (COX1, 16S rDNA) and the nuclear region (ITS1), was used in this analysis. The approach was implemented separately-three times, firstly by assigning individuals to minimal clusters based on current taxonomy (taxonomy approach), secondly by assigning individuals to minimal clusters based on the monophyletic groups supported by the phylogenetic analyses (monophyly approach) and thirdly using the minimal clusters inferred by the mPTP analyses (mPTP approach). During the input file setup in Beauti v.2.6.6, the BEAST Model Test (Bouckaert and Drummond, 2017) option was selected for nucleotide model assignment in partitions. The dataset was partitioned as described in Table S1. Regarding the remaining priors, the birth death model was used to estimate the species tree [priors: collapse height = 0.0001, collapse weight = 0.5 using a beta prior]. For the coalescent analysis the ploidy was set to 1 for the ITS1 partition and 0.5 in all mtDNA partitions. In the clock model, a relaxed lognormal clock prior was enforced. This model was chosen since the assumption of a constant substitution rate in an analysis involving highly divergent species, would be too constraining. The relative clock rates of all the gene fragments were estimated and a lognormal (lower = 0.0, upper = 1.0) prior was assumed for these. The MCMC analysis was run for 10^8 generations, saving the results every 10^5 generations. Convergence of the analysis was evaluated through the inspection of the effective sample sizes (ESS) using Tracer v.1.7.1 (Rambaut et al., 2018) and the analysis was considered to have reached convergence when the ESS (after discarding the burnin) attained values greater than 200. Finally, the most supported number of distinct clusters was estimated using SpeciesDelimitationAnalyser v1.8.0 (Jones, 2017) through the analysis of the MCMC tree samples with a burn-in of 25%. The default collapse height of 0.0001 was used.

BPP v.4.4.0 (Flouri et al., 2018) was used to validate the number of species inferred through the previous species delimitations methods. BPP is a multi-locus, coalescent-based method that makes use of prior demographic information and divergence times and estimates the posterior distribution for different species delimitation suggestions. The number of species delimited from each of the methods described above, was different. Therefore, to run the BPP we formatted the input file to reflect the suggestion of each of the three delimitation approaches (taxonomy approach, monophyly approach, mPTP approach) that were implemented in STACEY as well. Outgroup taxa were not included in the BPP analyses. In all BPP runs, the two mtDNA loci were treated as a single locus that was analyzed jointly with the nuclear locus. Therefore, as suggested in Flouri et al. (2018) both the “heredity” and the “locusrate” control variables were properly set in all runs. We implemented the A10 algorithm using as (fixed) guide tree the BI phylogenetic tree previously generated with all three gene fragments (concatenated dataset). The finetune option was enforced in the analysis and several preliminary runs were performed before choosing the most appropriate initial priors. The analyses with the most appropriate priors were performed twice to ensure convergence. In each run, the number of generations was 10^6, sampling frequency was set to 2 and a 10% burn-in was applied. The guide phylogenetic tree generated from each of the three different BPP analyses performed, with the posterior probability for presence of nodes was viewed with FigTree v.1.4.3.

2.5. *Divergence time estimates*

To reconstruct a dated phylogeny of the Iuridae we used BEAST v.1.10.4 (Suchard et al., 2018) and the concatenated dataset (Table S1). The dataset was partitioned per locus, therefore there were three different partitions in total (COX1, 16S rDNA and ITS1). PartitionFinder and the Bayesian Information Criterion (BIC) was used in the model fitting process. Substitution and clock models were unlinked across the partitions. An uncorrelated relaxed molecular clock was applied in each partition. The clock rates applied were retrieved from scorpion literature. More specifically the clock rate implemented for COX1 (mean = 0.0079, standard deviation = 0.00146) was the one reported for *Iurus* in Parmakelis et al. (2006b), whereas for 16S rDNA, the rate (mean = 0.005, standard deviation = 0.00270) used in Loria and Prendini (2020) was applied. The rate of ITS1 was estimated relatively to the rates applied for COX1 and 16S rDNA. In applying the rates, our aim was to ensure that 95% of the distribution would include minimum and maximum values of the COX1 and 16S rDNA loci in scorpions. To generate the ultrametric tree, two independent runs with a chain length of 10^8 were executed and sampling was performed every 10^4 iterations. In each run, convergence was evaluated through Tracer v.1.7.1 (see convergence reasoning in 2.4). Independent runs were combined using LogCombiner v.1.10.4, after discarding the first 10% of each run as burn-in. The MCC tree was generated using TreeAnnotator v.1.10.4 and viewed using FigTree v.1.4.3.

2.6. *Ancestral range estimation*

Ancestral range reconstruction for the time-calibrated phylogenetic tree was implemented using the BioGeoBEARS v. 1.1.2 package in R v. 4.1.2. The input files and analyses settings followed the instructions provided for the package that are available in https://phylo.wikidot.com/biogeobears. Outgroups were not included in the analyses and each species was represented in the tree with a single lineage. The R package ape v.5.6-1 was used to prune the time-calibrated tree. The four areas (A, B, C and E, Fig. 5) used for Turkey, are located within bioregions identified in the area in previous studies of Turkish faunal and floral elements (Casale and Taglianti, 1999; Kornilios et al., 2011; Kotsakiozi et al., 2018; Lopez-Pujol et al., 2016; Noroozi et al., 2019; Şenkul and Kaya, 2017; Skourtanioti et al., 2016). It has to be noted here, that area A besides the areas of mainland Turkey, includes the Greek islands of Rhodes and Megisti (Kastelorizo) as well. Similarly for Greece, the three areas (D, F and G, Fig. 5) used in the ancestral area reconstruction analyses have been identified in previous faunal studies from the region (Kornilios et al., 2009; Kotsakiozi et al., 2018; Parmakelis et al., 2013; Parmakelis et al., 2005; Parmakelis et al., 2006a; Parmakelis et al., 2006b; Skourtanioti et al., 2016). Each terminal species was scored as present or absent in the predefined areas for Turkey and Greece. The maximum number of areas a species can occupy was limited to two. Two model comparisons analyses were performed, the first involved the comparison of the models BAYAREALIKE, DEC, and DIVALIKE, and the second one involved the same models with the addition of the parameter jump-dispersal “j”, which allows for a founder-event speciation to be evaluated as well (Matzke, 2014).

3. Results

3.1. *Sequence data*

We successfully generated sequence data for all three gene fragments targeted (COX1, 16S rDNA, ITS1) in all the specimens included in the analyses. Following the removal of low-quality sequencing signals from the 5′ and 3′ ends of the amplified fragments, we obtained the loci datasets described below. The COX1 sequence dataset was comprised of 609 bp. Out of these, 203 were variable and 163 were parsimony informative. In 16S rDNA, there were 200 and 137 out of 531 bp that were variable and parsimony-informative, respectively. The majority of the generated sequences of the targeted nuclear region included the whole sequence of the ITS1 region and only a few of them included very small parts of either 18S rDNA or 5.8S. The aligned ITS1 dataset was 510 bp in length and included 169 variable and 108 parsimony-informative sites. At this point we must note that a single ITS1 “allele” was retrieved in all Iuridae specimens. Therefore, no “intra-specimen” ITS1 variation was recorded.

The levels of sequence divergence based on the p distance metric, between individual Iuridae sequences ranged between 0% and 17.0%, 0% and 21%, 0% and 22%, for COX1, 16S rDNA and ITS1, respectively.

3.2. *Phylogenetic analyses*

The results of the phylogenetic analyses based on the concatenated dataset are presented in Fig. 3. This analysis provided an almost fully

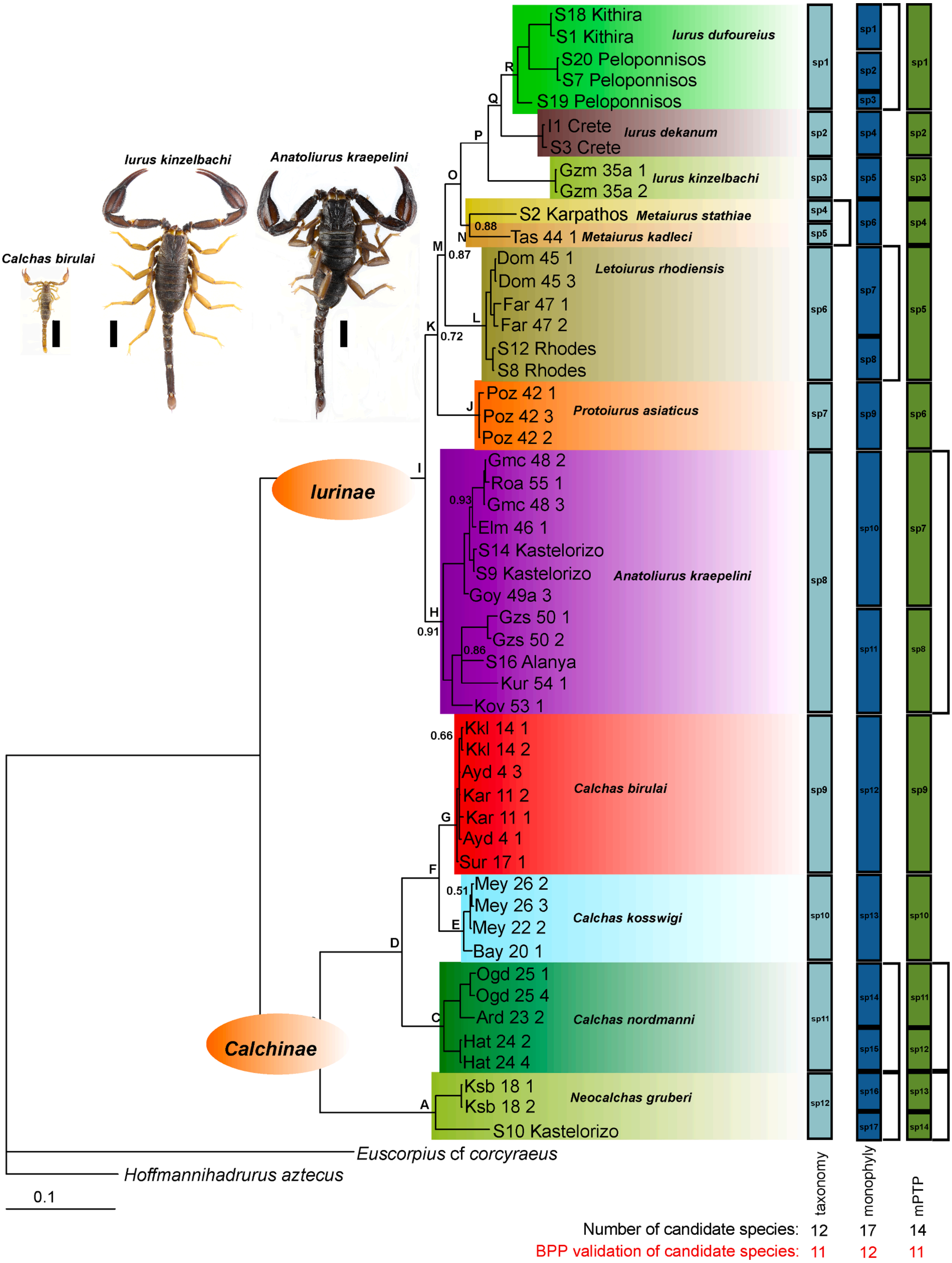

Fig. 3. Fifty percent majority-rule consensus tree of the Bayesian Inference (BI) analysis performed with MrBayes (the scale bar represents nucleotide substitutions per site). Number next to the nodes represent the posterior probabilities (only values below 0.95 are shown). Major nodes of the phylogenetic tree are named using the letters A to R. Although not shown, the Maximum Likelihood analysis branch support (three branch support methods) is highly congruent with that of the BI analysis. The distribution of Iuridae taxa into candidate species as inferred by the various species delimitation methods (one column per method), is indicated on the side of the BI analysis tree. The total number of species delimited by each method is shown at the bottom of each column. Species assignments based on taxonomy as revised herein, are shown. The number of species validated for each species delimitation method by the BPP analysis is also reported. Species not validated (i.e., collapsed into a single species) by the BPP analysis are included in brackets. The embedded picture shows three iurid species aiming to highlight the size differences between the Iurinae and the Calchinae. Scale bar is 10 mm.

resolved phylogenetic tree, thus is the one presented and commented upon. The majority-rule consensus BI tree is depicted in Fig. 3 and only posterior probabilities below 0.95 are indicated on the nodes. Concerning the major cladogenetic events, the topology of the ML analysis was identical to that of the BI analysis. The branch support between the BI and the ML methods was largely congruent in most of the nodes. However, it is evident that there are some nodes that were not resolved in either of the analyses. The respective statistical support of the BI (MrBayes) analysis is indicated on the nodes of the tree presented in Fig. 4, whereas the corresponding values from the ML (IQTREE2) analysis (three different methods of branch support analysis), are presented in Table S2. The major nodes of the phylogenetic tree are named using the letters A to R.

3.3. Species delimitation

Based on mPTP that relied solely on the mtDNA BI tree, the number of candidate species of Iuridae is 14 and as already mentioned, based on the BI tree, the monophyletic groups inferred are 17. At the same time, according to the current taxonomy of Iuridae, 12 species are present on the phylogenetic tree. The three different analyses performed using the STACEY method have not been able to reject any of the candidate species of any of the analyses. Thus, according to STACEY, all 12 morphologically identified clades (taxonomy approach) are candidate species. The same finding holds both for the 17 candidate species identified by adopting the monophyly approach and the 14 species identified by the mPTP approach.

The species validation approach using BPP provided maximal support (pp = 1.00) to the majority of the species suggestions of each delimitation approach (taxonomy approach, monophyly approach, mPTP approach). At the same time, some species suggestions were identified as not likely valid. The posterior probability threshold for not validating a species suggestion was set to 0.75. More specifically, in the taxonomy approach out of the 12 species, 11 were validated, thus the presence of one (1) species was not supported by the data. In the monophyly approach out of the 17 species 12 were validated. Finally, in the mPTP approach the presence of 11 out of the 14 candidate species were supported.

The results of the BPP analyses are presented in detail in Fig. 3. Following the validation of species suggestions using BPP, a general consensus regarding the number and the composition of species emerged. However, there was also one case in which the discrepancy persisted. This case regarded the species *Protoiurus kraepelini* (von Ubisch, 1922), that based on the monophyly criterion it could be split into two separate taxa (see Fig. 4). This split suggestion was not rejected by STACEY or the BPP analyses that were performed based on the monophyly criterion of clustering individual specimens. In contrast, this split was not supported when BPP validation analyses was implemented on the species delimitation suggestion of the mPTP method that included this split (Fig. 4). At the same time, according to morphology all *P. kraepelini* specimens of our study form a single clade.

3.4. Divergence time estimates

The time-calibrated tree inferred using BEAST is presented in Fig. 4. The geological periods indicated in the time scale bar are according to the most recent version (2021) of the International Chronostratigraphic Chart (https://www.stratigraphy.org). The tree is well resolved and the topology is fully congruent to that of the phylogenetic analyses based on the concatenated dataset, presented in Fig. 3. Based on the time estimates, the cladogenetic event leading to Iurinae and Calchinae occurred 36 mya. On the other hand, the radiations within Iurinae and Calchinae initiated 18 and 27 mya, respectively.

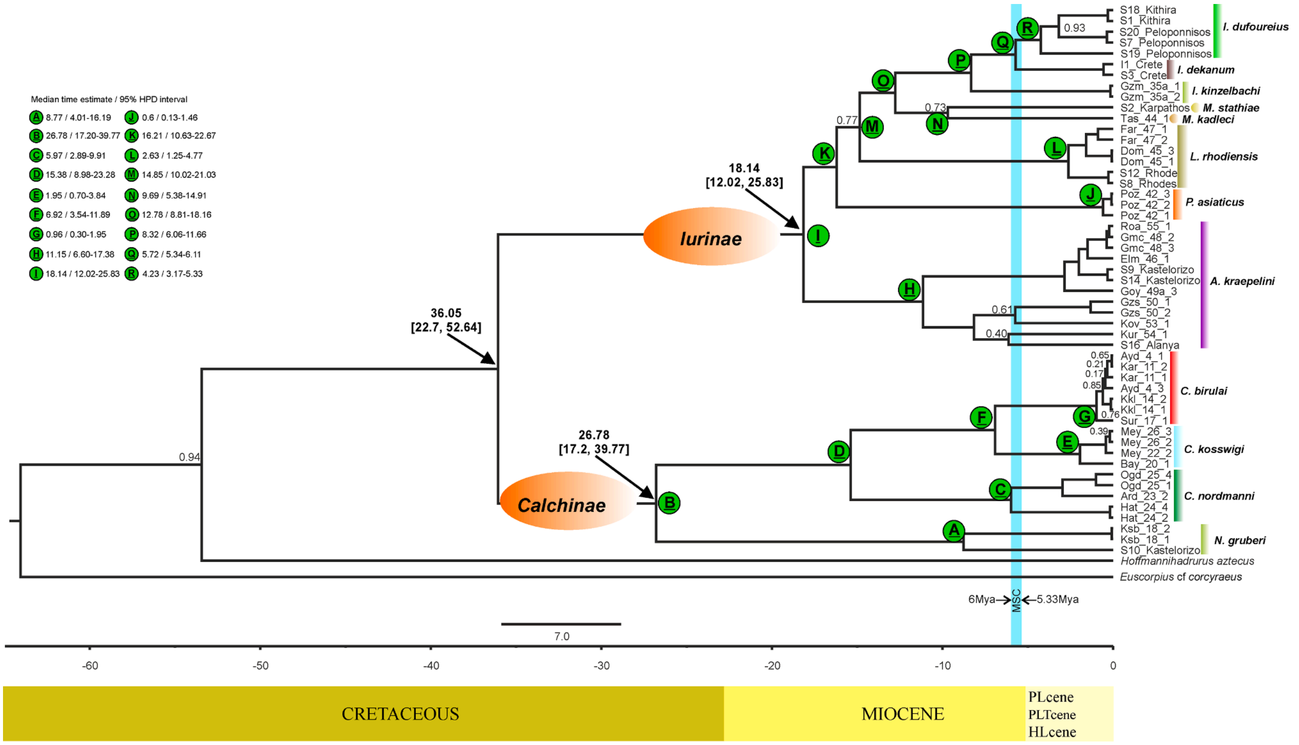

Fig. 4. Iurid multi-locus species tree chronogram inferred using BEAST v 1.10.4. The scale bar represents millions of years. Numbers on nodes correspond to the posterior probabilities. Major nodes are named using the letters A to R as in Fig. 3. Specimens were assigned to species/clades according to the validated Iurid species of the BPP analyses performed. The time axis (median ages) is indicated at the bottom. The median time estimates (mya) and the 95% HPD intervals for each node of the tree are shown in the inset of the figure. The Messinian Salinity Crisis time period is also shown on the figure.

3.5. Ancestral range estimation

The DEC + J model was identified as the most appropriate for the dataset (Table 2). Based on this model, the ancestor of both Calchinae and Iurinae occupied the geographic areas A, B and C. Based on the DEC + J model multiple dispersal and vicariant events, together with within areas speciation events, have shaped the present-day distribution of the iurids in this region. The range-inheritance events, are presented in Fig. 5.

4. Discussion

4.1. Species delimitation and taxonomic implications

The resulting DNA phylogeny revealed a complex topology, hitherto unsuspected even from detailed morphological studies of Iuridae. There are 17 (seventeen) monophyletic groups (clades) strongly supported by the analysis. The relationships between these clades are very well resolved in most of the cases. However, there is also a small number of clades that are ambiguously related to each other as indicated by the support values that are below 0.95 (or 95% bootstrap support). Consequently, based on the results of the species delimitation analyses and the validation of species suggestions with BPP, the consensus of the valid Iuridae species present in our data is 11. At this point we must note that there is a plethora of methods for delimiting species using molecular datasets. Each of these, has advantages, disadvantages and limitations (Scornavacca et al., 2020). All delimitation methods rely on a number of simplifying assumptions, any one of which could be violated in a particular study system (Carstens et al., 2013). For these reasons we followed a conservative approach by applying different delimitation analyses to our data and placing our trust in delimitations that appeared congruent across them. Consequently, the consensus number of species in our study, originates after accepting as valid only the species supported by a minimum of two out of the three (taxonomy approach, monophyly approach, mPTP approach) different implementations of the BPP validation method. These 11 species include the ones already described, except the two nominal species *Protoiurus kadleci* and *P. stathiae* that appear as belonging to a single species.

4.2. Taxonomic changes introduced in this work

Based on our findings, taxonomic changes are deemed necessary for the Iuridae. All the taxonomic changes introduced in this work, are summarized in Table S3. We restore the subfamily Calchinae Birula, 1917, **stat. n.** from synonymy with Iurinae Thorell, 1876. Three new generic names are established to resolve the paraphyletic genus *Protoiurus*. For further details on the subordinate taxa, see: Kovařík et al. (2010); Soleglad et al. (2012); Yağmur et al. (2015a, 2015b).

Anatoliurus gen. n. Type species: *Iurus kraepelini* von Ubisch, 1922.

http://zoobank.org/urn:lsid:zoobank.org:act:BA76225F-12EC-47F5-813D-604B2267D708

DIAGNOSIS (based on Kovařík et al. (2010); Soleglad et al. (2012); Yağmur et al. (2015b)). Large sized scorpions, up to 100 mm. Pectinal tooth counts 10–16 in males, 10–14 in females. Chelal movable finger lobe in adults located on mid-finger or distally, lobe ratio 0.44–0.64; proximal gap of fixed finger present in adult males; movable finger of adult males conspicuously curved; chelal palm of adult males short, deep and highly vaulted; number of inner denticles (ID) of chelal movable finger, 11–14; hemispermatophore type 1b (*A. kraepelini*) or type 1a (*A. kumlutasi*).

Etymology: the generic name is given after the Anatolian Peninsula, or Asia Minor.

Subordinate taxa: *Anatoliurus kraepelini* (von Ubisch, 1922), **comb. n.**, *A. kumlutasi* (Yağmur et al., 2015a, 2015b), **comb. n.**

Distribution. Turkey (Antalya, Isparta, Konya, Karaman, Mersin, and Muğla Provinces); Greece (Megisti Island).

Letoiurus gen. n. Type species: *Protoiurus rhodiensis* Soleglad et al., 2012.

http://zoobank.org/urn:lsid:zoobank.org:act:1914D39E-CDDB-4B6B-AFED-CE84ED880A06

DIAGNOSIS (based on Soleglad et al., 2012). Medium sized scorpions, 85 mm. Pectinal tooth count 10–14 in males, 8–12 in females. Chelal movable finger lobe in adult males located on basal half, lobe ratio 0.44–0.49; a subtle weak proximal gap on fixed finger present in adult males; movable finger of adult males essentially straight, not highly curved; number of inner denticles (ID) of chelal movable finger, 12–14; hemispermatophore type 1a.

Etymology: the generic name is derived from Greek Λητώ, *Leto,* the Olympian goddess, mother of twins Artemis and Apollo. Leto was worshipped in ancient Lycia (now Muğla), where a famous temple site exists, the Lycian Letoon.

Subordinate taxa: *Letoiurus rhodiensis* (Soleglad et al., 2012), **comb. n.**, (monotypic genus).

Distribution. Greece (Rhodes Island); Turkey (Muğla Province).

Metaiurus gen. n. Type species: *Protoiurus stathiae* Soleglad et al., 2012.

http://zoobank.org/urn:lsid:zoobank.org:act:032524C3-53BC-4941-B612-B7018985FD08

DIAGNOSIS (based on Kovařík et al. (2010); Soleglad et al. (2012); Yağmur et al. (2015a)). Medium to large sized scorpions, 75–105 mm. Pectinal tooth counts 9–15 in males, 10–14 in females. Chelal movable finger lobe in adult males located on mid-finger or distally, lobe ratio 0.55–0.65; a conspicuous proximal gap of fixed finger present in both adult males and females; movable finger of adult males essentially straight, not highly curved; number of inner denticles (ID) of chelal movable finger 11–14; hemispermatophore type 1a.

Etymology: the generic name is derived from Greek μετά *meta,* “after, beyond”.

Subordinate taxa: *Metaiurus kadleci* (Kovařík et al., 2010), **comb. n.**, *M. stathiae* (Soleglad et al., 2012), **comb. n.**

Distribution. Greece (Karpathos Island: *M. stathiae*); Turkey (Antalya and Mersin Provinces: *M. kadleci*).

4.3. Taxonomic composition of Iuridae Thorell, 1876

The current taxonomic composition includes two subfamilies, seven

Table 2
Statistical results of the different models compared in in ancestral range estimation of the iurid scorpions of Eastern Mediterranean. The models were DEC, DIVALIKE and BAYAREALIKE. The models were compared to each other and the respective ones involving an additional founder effect (j) parameter. The likelihood of each model (lnL), the number of parameters in each model, a dispersal parameter (d), an extinction parameter (e), the founder effect parameter (j), corrected Akaike Information Criterion (AICc), and corrected Akaike Information Criterion weight (AICc_wt) are provided. The most probable model is written in italics.

	LnL	Number of Parameters	d	e	j	AICc	AICc_wt
DEC	−35.856	2	0.012	0.020	0.000	77.045	0.000
DEC + J	−26.413	3	0.001	0.000	0.141	61.825	0.805
DIVALIKE	−34.599	2	0.009	0.008	0.000	74.532	0.001
DIVALIKE + J	−28.106	3	0.002	0.000	0.140	65.212	0.148
BAYAREALIKE	−37.591	2	0.017	0.046	0.000	80.516	0.000
BAYAREALIKE + J	−29.298	3	0.001	0.000	1.000	67.597	0.045

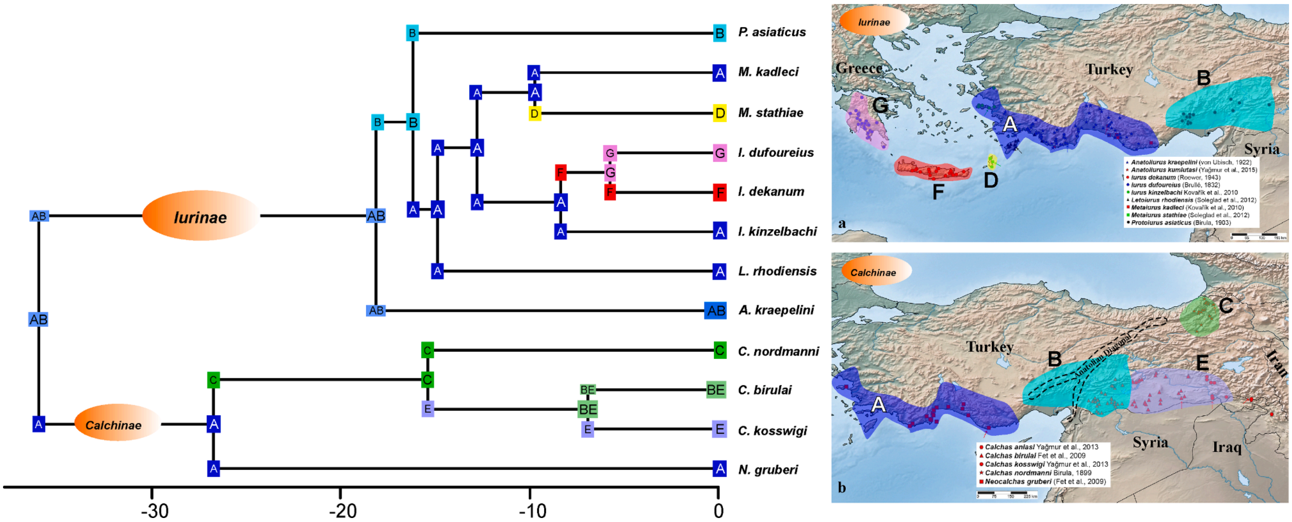

Fig. 5. Ancestral range estimates of the East Mediterranean Iuridae using DEC + J. The distributional areas A to G are presented in the embedded maps (map a: Iurinae, map b: Calchinae). The ancestral range estimates were performed with BioGeoBEARS, based on the chronogram generated with BEAST. Single most probable ancestral range is mapped at each node. Areas at corner positions represent the geographic range immediately after a cladogenetic event. The Anatolian Diagonal (ADL) is indicated with the dashed line.

genera and 14 species (Table 1).

Subfamily Calchinae includes two widely disjunct genera, of which monotypic *Neocalchas* is found in southwestern Anatolia and on the coastal Greek islands of Megisti and Samos. The second genus *Calchas* includes four species: the type species *C. nordmanni* with a disjunct range in the northeastern Anatolia (Artvin and Erzurum Provinces) and three arid species from southeastern Turkey (*C. anlasi, C. birulai*, and *C. kosswigi*). The single known population in northern Iraq is tentatively assigned to *C. anlasi.*

Subfamily Iurinae includes five genera: *Anatoliurus* **gen. n.**, *Iurus*, *Metaiurus* **gen. n.**, *Protoiurus*, and *Letoiurus* **gen. n**. *Anatoliurus* includes two species. While *A. kumlutasi*, **comb. n.,** is known only from a single cave, *A. kraepelini*, **comb. n.,** is widespread in the southwest to south-central Turkey (also found on the Greek island of Megisti). Three species of *Iurus* are heavily disjunct: two endemic Greek species are found in the Peloponnese and Kythira (*I. dufoureius*) and Crete (*I. dekanum*); the third, *I. kinzelbachi*, in western Turkey and the Greek island of Samos. *Metaiurus* **gen. n.,** includes two disjunct species: *M. stathiae*, **comb. n.,** from the island of Karpathos, and a localized *M. kadleci*, **comb. n.,** from Turkey. The monotypic *Protoiurus* includes *P. asiaticus* from the eastern Turkey, separated from other iurines by the higher elevations of the Taurus Mountains. Another monotypic genus, *Letoiurus,* includes *L. rhodiensis*, **comb. n.,** from the Greek island of Rhodes and southwestern Turkey (Muğla Province; first record in Turkey).

4.4. *Time frame of differentiation and biogeography of subfamilies and delimited species*

An ancient division of Iuridae into subfamilies Iurinae and Calchinae is strongly supported by our analysis: both form monophyletic groups. There are no fossils of Iuridae, and we can only speculate on their common Cenozoic ancestry dated not later than 36 mya, at the end of the Eocene epoch. At the end of the Eocene, the Anatolian plate has already been formed (Popov et al., 2004a; Popov et al., 2004c) and served as the diversification area of the family.

According to the ancestral range estimate analysis, the suggestion of Parmakelis et al. (2006b) for a westward dispersal of *Iurus* species, is validated. However, the sequence of events in both the westward and the eastward direction of dispersal of the iurids, are complex and entail a crucial role of the Aegean insular areas in shaping the present-day distributional patterns of both insular and mainland species. According to the supported ancestral ranges hypotheses, and focusing on the Calchinae, the differentiation of the family initiated in area A approximately 27 mya. One of the derived lineages maintained the distributional range of the ancestor and gradually led to *Neocalchas gruberi*. The other lineage gradually reached far to the northeast part of the Turkish mainland in area C. Region C resides within the Pontic Mountains, a region that has been identified as a major area of endemism in Anatolia for both plant and animal species (Casale and Taglianti, 1999; Lopez-Pujol et al., 2016; Noroozi et al., 2019; Şenkul and Kaya, 2017). *C. nordmanni* was the first species to diverge approximately 16 and maintained the ancestral distributional area (C). The ancestor of *C. birulai* and *C. kosswigi* followed a southwards dispersal route from C to area E (Şanliurfa-Idil region, west of the Amanos Mountain) and approximately 8 mya extended its distributional range to include area B (part of the Anatolian Diagonal, ADL). The ancestor lineage with the BE distributional range differentiated to species *C. birulai* and *C. koswigi*. The latter was constrained in area E, whereas *C. birulai* maintained the ancestral range (BE). The ADL is a line of mountain ranges that run from the south of Gümüşhane – Bayburt in the north, southwest across Turkey to the Taurus Mountains (Ekim and Guner, 1986). Several previous studies of species distribution and regional composition have suggested that, together with the Tertiary history of Turkey, the ADL might be responsible for breaks in distributions at both specific and generic levels (Mutun, 2010). According to several studies, the ADL played a critical role for the distribution of many species (Çiplak et al., 1993; Meijers et al., 2020; Mutun, 2010; Skourtanioti et al., 2016) since late Miocene. As evidenced here, the role of ADL in shaping the distributional patterns of animal taxa is verified in the case of the Calchinae.

Regarding the Iurinae, the ancestral range included areas A and B. Area A is actually the southern part of Turkey and also includes the Greek islands of Rhodes and Megisti (Kastelorizo). This area represents the Mediterranean-Aegean ecoregions of Turkey (Casale and Taglianti, 1999). Area B belongs to the ADL as described above. The first Iurinae species to diverge 18 mya is *Anatoliurus kraepelini* that is the most widespread species of the iurids. This species maintained the ancestral range (AB) of distribution. Approximately 16 mya a cladogenetic event occurs within area B, and one of the derived lineages maintains the ancestral distribution area B and eventually gives rise to *Protoiurus asiaticus*. The second derived lineage is found in area A. From there, through several consecutive ancestral range-inheritance-events and quite limited dispersal and vicariant events, gives rise to three Iurinae genera (*Iurus*, *Letoiurus*, *Metaiurus*) and six species altogether. Most of the dispersal events relate to the westward movement of some lineages into areas of the Aegean Archipelago (Fig. 5). In Miocene, the faunal exchange between Asia and the Balkans became possible around 11 Ma (Fassoulas, 2018). At that time, connection of Anatolia, via the South Aegean Arc, to modern Crete and Peloponnese, could have produced two most recently derived western species of *Iurus:* the island endemic *I. dekanum* of Crete, and the only iurid that reached the European mainland, *I. dufoureius* of Peloponnese and Kythira Island (**Node R**). The divergence between *I. dekanum* and *I. dufoureius*, dated at about 5.7 Ma (Lower Miocene) fits very well to the time period of the Messinian Salinity Crisis (Krijgsman et al., 2018; Krijgsman et al., 1999), after which Crete and Peloponnese were never connected again. Based on our findings, it seems that the genus (and the family) either never crossed the Isthmus of Corinth to the north—or did cross it and eventually went extinct.

The present-day distributional patterns of the Iurinae and Calchinae besides historical reasons, are most certainly due to ecological requirements of the species as well. Between the Iurinae and Calchinae, a contrasting pattern of morphological (likely adaptive) evolution has been documented: all members of the Iurinae are large-sized animals (75–100 mm adults), while all the Calchinae are small scorpions (25–35 mm adults). Ecological differences between the subfamilies have also been recorded during our field surveys: while species of both subfamilies are found in diverse habitats from the sea level to high altitude (2100 m asl in *Calchas nordmanni*, 1300 m in *Protoiurus asiaticus*), clearly arid adapted taxa are present only in the Calchinae, with three species (*C. anlasi, C. birulai* and *C. kosswigi*) inhabiting dry semidesert areas of SE Anatolia. The two remaining species of Calchinae live either in areas of Mediterranean climate (*Neocalchas gruberi*) or in valleys of north-eastern Turkey with a Mediterranean type of microclimate (*Calchas nordmanni*). Among the Iurinae, most species are found in areas of Mediterranean climate but not in arid habitats, and they are notably missing from the most of SE Anatolia. The Iurinae, their large size notwithstanding, are commonly found in caves and human related habitats. A formal investigation of the issue of ecological differentiation between the species of the subfamilies must be performed to substantiate the claims presented herein. For this reason, detailed distributional data of the species have been collected and environmental niche modelling analyses will be presented in a forthcoming publication.

In the following lines, we are presenting a short evolutionary story for each species in the phylogeny and try to interpret it on the grounds of both palaeogeography and ecology.

The last common ancestor (LCA henceforth) of the current taxa belonging to the Calchinae (**Node B,** Fig. 4) is dated (median value) 27 mya, i.e., in the Late Oligocene. The most basal taxon among Calchinae (**Node A,** Fig. 4) is the monotypic genus *Neocalchas* with its sole species, *N. gruberi* (SW Anatolia; Megisti and Samos Islands). It represents the most ancient relict clade identified among iurid scorpions. *N. gruberi* is found in habitats of the Mediterranean coast, with mild Mediterranean climate, i.e., dry summers and mild, wet winters. A separate clade on the Megisti (Kastelorizo) Island is indicated compared to mainland Anatolian population (Antalya Province). At this time (27 mya), the Anatolian plateau was more or less an island with a possible connection through a land bridge with the Elbutz-Kopetdagh land, which corresponds to Central Iran today (Popov et al. (2004b), Map 3). The common ancestor of Calchinae (Node B, Fig. 4) seems to have lived at that time. From 20.5 to 15 mya, Anatolia was separated of Elbutz-Kopetdagh land by sea (Popov et al., 2004b, Maps 4 and 5), and this is when *N. gruberi* (Node A) must have differentiated from *Calchas* spp. (Nodes C, E, G, Fig. 4).

Node D (Fig. 4**)** leads to the clade representing the genus *Calchas*. Divergence of its species is dated around 15 Ma (Middle Miocene). Since 15 mya, Anatolia and the land of Elbutz-Kopetdagh was forming a united land mass (Popov et al. (2004b), Maps 5–8). These two areas were separated again at 8.5–7 mya (Popov et al. (2004b), Maps 8), and this is when Node F (Fig. 4) (*C. kosswigi* and *C. birulai*) most probably differentiated from Node C (*C. nordmanni*).

Calchas nordmanni (type species of the genus), is found in NE Anatolia in the humid valleys of the eastern Black Sea region and it is an ancient, relict species. It is separated by the mountain ranges of Caucasus and Taurus from other Anatolian members of the genus. Topology of three studied populations (**Node C,** Fig. 4) indicates a separate clade in the very northeastern (Hatila Valley) limit of the species' range, close to the border with Georgia (where *Calchas* has not been recorded). *C. nordmanni* is orophylic and found up to 2100 m asl but not in the coastal areas of the eastern Black Sea region.

Node F (Fig. 4**)** represents the common ancestor of two clearly arid SE Anatolian species, *C. kosswigi* and *C. birulai*. Divergence of those is recent, dated at approximately 7 mya (Upper Miocene). This clade probably originated during the period that the Anatolian Peninsula started experiencing aridization. This period is placed within the Late Miocene-Pleistocene (Huang et al., 2019; Meijers et al., 2018).

The species *Calchas kosswigi* is found only in Siirt and Sirnak Provinces, SE Turkey. Its sister taxon, *Calchas birulai*, is the most widespread *Calchas* species in the arid, semidesert SE Anatolia. Although these species occupy arid areas, they are not xerophilic. They are active only during the humid and cool period, between February and May.

Node I represents the LCA of the current taxa belonging to the subfamily Iurinae, and is dated around 18 Ma (Early Miocene). The most important event at this point, or even earlier, is the appearance of gigantism (see embedded picture in Fig. 3), since all Iurinae exhibit very large adult size (300–400% larger than in *Calchas* and *Neocalchas*). This event most likely occurred in what is now Southern Anatolia, as the subfamily never dispersed to the northern part of the peninsula, possibly due to the barrier of the Kırşehir Massif between the Pontides and Tauride-Anatolide Continent (Licht et al., 2017). New clades of the "giant race" successfully radiated leading to several species still resident there, and eventually dispersed to the west across the Aegean Sea. We can observe a monophyly of the derived genus *Iurus* (**Node P**) while the genus *Protoiurus* was revealed as being strongly paraphyletic. To resolve this paraphyly, three new genera are established: *Anatoliurus* **gen. n.**, *Metaiurus* **gen. n.**, and *Letoiurus* **gen. n.** (see above for formal taxonomy).

Node H leads to the most basal of all Iurinae species (formerly in *Protoiurus*), *Anatoliurus kraepelini* **comb. n.** (several populations, with deep internal structure). Its divergence from other taxa is dated at about 11 Ma (Late Miocene). It is found predominantly in southern Anatolia, and also on the coastal Greek island of Megisti (Kastelorizo). It is the most widespread species of Iuridae (Fig. 1). To resolve the paraphyly, we establish for this clade a new generic name *Anatoliurus* **gen. n**. We also tentatively assign to this genus the closely related rare Anatolian cave species *A. kumlutasi* **comb. n.**

Node K leads to *Protoiurus asiaticus*, the easternmost species of Iurinae. Its divergence is dated at about 16 Ma (Middle Miocene). With a rather limited range in SE Anatolia, it is the most orophilic and cold-tolerant species of the subfamily Iurinae, rising up to 1300 m in the Taurus Mountains. Since this is the type species of the genus *Protoiurus,* other *Protoiurus* spp. are herein placed in three new genera. The genus *Protoiurus* s.str. therefore, becomes monotypic.

Node M leads to the species *Letoiurus rhodiensis* **comb. n.** (Rhodes Island; western Anatolia: Muğla: first record) (formerly placed in *Protoiurus*). Its divergence is dated at about 15 Ma (Middle Miocene). *Letoiurus* **gen. n.** is a monotypic genus, an Anatolian relict. Its refugial population on Rhodes could have been isolated 2 mya (Pleistocene) when the island was for the last time connected to the Anatolian mainland (Beerli et al., 1996; Gantenbein and Largiadèr, 2002).

Node N leads to the rare species *Metaiurus kadleci* **comb. n.** (with a limited range in southern Anatolia) and an island relict *M. stathiae* **comb. n.** (Karpathos Island), both formerly placed in *Protoiurus*. Intriguingly, these two species were grouped into a single species by our species delimitation analyses. Still, there is 9% sequence difference in

COX1 gene and an equally high divergence in the other two markers. Therefore, at this moment we prefer to refrain from synonymization of these two widely allopatric taxa (which differ quite significantly in morphology; see Soleglad et al. 2012). To resolve paraphyly, we establish for this clade a new generic name *Metaiurus* **gen. n.** According to the time-estimate analysis (Fig. 4) the isolation of *M. stathiae* on Karpathos occurred during the Lower Miocene (~10 mya). Karpathos was an island during the Miocene and it remained so until it was joined with Anatolia through Rhodes in the Early Pliocene (Daams and Van Der Weerd, 1980). In the Late Pliocene, the island of Karpathos was almost totally submerged, and has remained isolated since then (Böger and Dermitzakis, 1987). The lineage of Karpathos probably survived in the island in areas that were not submerged.

Node P represents the LCA (dated around 8 Ma, Lower Miocene) of three *Iurus* species. Therefore, according to the phylogenetic analysis, the genus *Iurus* is monophyletic, originates from Anatolia, and its basal species is a relict species, *I. kinzelbachi* of western Anatolia and the coastal Samos Island (Greece). The pattern of a relict Iuridae species being present in one Aegean Island is evident as well in *Neocalchas* and *Anatoliurus* on Megisti, and in *Letoiurus* on Rhodes.

5. Conclusion

Iuridae, a relict East Mediterranean family, exhibits a long history of divergence, speciation, and adaptation. Our molecular datasets and analyses for the first time clearly confirm an ancient division into two clades, Calchinae and Iurinae, with their separate evolutionary history. Ancient patterns of isolation and dispersal are revealed. Both subfamilies are largely confined to the Anatolian peninsula and its few coastal islands; only the most derived genus *Iurus* has dispersed westward to Crete and Peloponnese. Based on phylogenetic data, we establish three new genera of Iurinae (*Metaiurus, Anatoliurus*, and *Letoiurus*), including taxa formerly classified under *Protoirus*. The genus *Neocalchas* emerges as one of the most ancient scorpion clades, with divergence time about 27 mya.

Funding

This research did not receive any specific grant from funding agencies in the public, commercial, or not-for-profit sectors.

CRediT authorship contribution statement

Aristeids Parmakelis: Conceptualization, Methodology, Resources, Investigation, Data curation, Formal analysis, Writing – original draft, Writing – review & editing, Visualization, Supervision, Project administration. **Domniki Dimitriadou:** Investigation, Formal analysis, Writing – review & editing. **Evdokia Gkigkiza:** Investigation, Formal analysis, Writing – review & editing. **Lydia Karampatsou:** Investigation, Formal analysis, Writing – review & editing. **Iasmi Stathi:** Conceptualization, Resources, Investigation, Writing – review & editing. **Victor Fet:** Conceptualization, Resources, Investigation, Writing – original draft, Writing – review & editing. **Ersen A. Yağmur:** Conceptualization, Resources, Writing – review & editing. **František Kovařík:** Resources, Writing – review & editing.

Declaration of Competing Interest

The authors declare that they have no known competing financial interests or personal relationships that could have appeared to influence the work reported in this paper.

Acknowledgements

We would like to thank two anonymous reviewers and the editor of MPE, for providing comments that greatly improved the manuscript. We are especially thankful to Michael E. Soleglad for his enormous contribution to the modern understanding of the remarkable Iuridae. Authors would like to thank Dr Charalampos Fassoulas for providing comments on issues of palaeogeography of the study region. We are also grateful to all colleagues who over the years kindly loaned and shared rare comparative material, information, and literature on Iuridae, including but not limited to: Abdulmuttalip Akkaya, Julia Altmann, Aziz Avcı, Petar Beron, Matt E. Braunwalder, Leoš Černý, Maria Chatzaki, Alberto Chiarli, Pierangelo Crucitti, Gökhan Çalışır, László Dányi, Salim Dudaklı, Jason Dunlop, Hakan Durmuş, Benjamin Gantenbein, Matthew Graham, Alexander Gromov, Jürgen Gruber, Christoph Hörweg, Jiří Hromádka, Peter Jäger, Dimitris Kaltsas, Hakan Karaoğlu, Rahşen S. Kaya, Altuğ Kızıltuğ, Ragnar Kinzelbach, Halil Koç, Kadir Boğaç Kunt, Petros Lymberakis, Moysis Mylonas, David Neff, Manolis Nikolakakis, Kurtuluş Olgun, Semih Örgel, Mehmet Özkörük, Manolis Papadimitrakis, Vera Pkhakadze, Dimitris Poursanidis, Carsten Renker, Petra Sierwald, Verena Stagl, Pavel Stoev, Georgios Tsiourlis, İsmail Hakkı Uğurtaş, Volkan Ülgezer, Valerio Vignoli, Mehmet Yalçın, Mehmet Zülfü Yıldız, Erol Yağmur, and Fatih Yeşilyurt, as well as the late Erich Kritscher, Viktor Krivokhatsky, Gary A. Polis, and Max Vachon.

Appendix A. Supplementary material

Supplementary material to this article can be found online at https://doi.org/10.1016/j.ympev.2022.107622.

References

Anisimova, M., Gil, M., Dufayard, J.F., Dessimoz, C., Gascuel, O., 2011. Survey of branch support methods demonstrates accuracy, power, and robustness of fast likelihood-based approximation schemes. Syst. Biol. 60, 685–699.

Ballesteros, J.A., Santibanez-Lopez, C.E., Baker, C.M., Benavides, L.R., Cunha, T.J., Gainett, G., Ontano, A.Z., Setton, E.V.W., Arango, C.P., Gavish-Regev, E., Harvey, M. S., Wheeler, W.C., Hormiga, G., Giribet, G., Sharma, P.P., 2022. Comprehensive species sampling and sophisticated algorithmic approaches refute the monophyly of Arachnida. Mol. Biol. Evol. 39.

Beerli, P., Hotz, H., Uzzell, T., 1996. Geologically dated sea barriers calibrate a protein clock for Aegean water frogs. Evolution 50, 1676–1687.

Böger, H., Dermitzakis, M.D., 1987. Neogene Paleogeography in the Central Aegean region. In: Proceedings of VIIIth International RCMNS Congress, Budapest 1985. Annals Hungarian Geological Institute, pp. 217–220.

Bouckaert, R.R., Drummond, A.J., 2017. bModelTest: Bayesian phylogenetic site model averaging and model comparison. BMC Evol. Biol. 17.

Bouckaert, R., Vaughan, T.G., Barido-Sottani, J., Duchene, S., Fourment, M., Gavryushkina, A., Heled, J., Jones, G., Kuhnert, D., De Maio, N., Matschiner, M., Mendes, F.K., Muller, N.F., Ogilvie, H.A., du Plessis, L., Popinga, A., Rambaut, A., Rasmussen, D., Siveroni, I., Suchard, M.A., Wu, C.H., Xie, D., Zhang, C., Stadler, T., Drummond, A.J., 2019. BEAST 2.5: An advanced software platform for Bayesian evolutionary analysis. PLoS Comput. Biol. 15.

Carstens, B.C., Pelletier, T.A., Reid, N.M., Satler, J.D., 2013. How to fail at species delimitation. Mol. Ecol. 22, 4369–4383.

Casale, A., Taglianti, A.V., 1999. Caraboid beetles (excl. Cicindelidae) of Anatolia and their biogeographical significance. Biogeographia 20.

Çiplak, B., Demirsoy, A., Bozcuk, A.N., 1993. Distribution of Orthoptera in relation to the Anatolian Diagonal in Turkey. Articulata 8, 1–20.

Daams, R., Van Der Weerd, A.V., 1980. Early Pliocene small mammals from the Aegean island of Karpathos (Greece) and their paleogeographic significance. Geol. Mijnb. 59, 327–331.

Ekim, T., Guner, A., 1986. The Anatolian Diagonal - Fact or Fiction. P. Roy. Soc. Edinb. B 89, 69–77.

Fassoulas, C., 2018. The geodynamic and paleogeographic evolution of the Aegean in the Tertiary and Quaternary: A review. Biogeography and Biodiversity of the Aegean. In Honour of Prof. Moysis Mylonas; Sfenthourakis, S., Pafilis, P., Parmakelis, A., Poulakakis, N., Triantis, KA, Eds, 25–46.

Fet, E.V., Soleglad, M.E., Kovařík, F., 2009. Etudes on iurids, II. Revision of genus *Calchas* Birula, 1899, with the description of two new species (Scorpiones: Iuridae). Euscorpius 82, 1–72.

Flouri, T., Jiao, X.Y., Rannala, B., Yang, Z.H., 2018. Species Tree Inference with BPP Using Genomic Sequences and the Multispecies Coalescent. Mol. Biol. Evol. 35, 2585–2593.

Francke, O., Soleglad, M.E., 1980. Two new *Hadruroides* Pocock, from Peru (Scorpiones, Vaejovidae). Occasional papers the museum Texas Tech University. Texas Tech University.

Gantenbein, B., Fet, V., Largiadèr, C.R., Scholl, A., 1999. First DNA phylogeny of the genus *Euscorpius* Thorell 1876 (Scorpiones, Euscorpiidae) and its bearing on the taxonomy and biogeography of this genus. Biogeographica 75, 59–72.

Gantenbein, B., Largiadèr, C.R., 2002. *Mesobuthus gibbosus* (Scorpiones: Buthidae) on the island of Rhodes — hybridization between Ulysses' stowaways and native scorpions? Mol. Ecol. 11, 925–938.

Guindon, S., Dufayard, J.F., Lefort, V., Anisimova, M., Hordijk, W., Gascuel, O., 2010. New algorithms and methods to estimate maximum-likelihood phylogenies: assessing the performance of PhyML 3.0. Syst. Biol. 59, 307–321.

Huang, S., Meijers, M.J.M., Eyres, A., Mulch, A., Fritz, S.A., 2019. Unravelling the history of biodiversity in mountain ranges through integrating geology and biogeography. J. Biogeogr. 46, 1777–1791.

Jones, G., 2017. Algorithmic improvements to species delimitation and phylogeny estimation under the multispecies coalescent. J. Math. Biol. 74, 447–467.

Kalyaanamoorthy, S., Minh, B.Q., Wong, T.K.F., von Haeseler, A., Jermiin, L.S., 2017. ModelFinder: fast model selection for accurate phylogenetic estimates. Nature Methods 14, 587.

Kapli, P., Lutteropp, S., Zhang, J., Kobert, K., Pavlidis, P., Stamatakis, A., Flouri, T., 2017. Multi-rate Poisson tree processes for single-locus species delimitation under maximum likelihood and Markov chain Monte Carlo. Bioinformatics 33, 1630–1638.

Kinzelbach, R., 1975. Die Skorpione der Ägäis. Beiträge zur systematik, phylogenie und biogeographie. Zoologische Jahrbücher, Abteilung für Systematik 102, 12–50.

Kinzelbach, R., 1980. Zur Kenntnis des kaukasischenSkorpions *Calchas nordmanni* Birula, 1899 (Scorpionida:Chactidae). Verh. Naturwiss. Ver. Hamburg (NF) 23, 169–174.

Kornilios, P., Ilgaz, etin, Kumluta, Yusuf, Giokas, S., Fraguedakis-Tsolis, S., Chondropoulos, B., 2011. The role of Anatolian refugia in herpetofaunal diversity: an mtDNA analysis of *Typhlops vermicularis* Merrem, 1820 (Squamata, Typhlopidae). Amphib-Reptilia 32, 351–363.

Kornilios, P., Poulakakis, N., Mylonas, M., Vardinoyannis, K., 2009. The phylogeny and biogeography of the genus *Zonites* Montfort, 1810 (Gastropoda: Pulmonata): preliminary evidence from mitochondrial data. J. Molluscan Stud. 75, 109–117.

Kotsakiozi, P., Jablonski, D., Ilgaz, Ç., Kumlutaş, Y., Avcı, A., Meiri, S., Itescu, Y., Kukushkin, O., Gvoždík, V., Scillitani, G., Roussos, S.A., Jandzik, D., Kasapidis, P., Lymberakis, P., Poulakakis, N., 2018. Multilocus phylogeny and coalescent species delimitation in Kotschy's gecko, *Mediodactylus kotschyi*: Hidden diversity and cryptic species. Mol. Phylogenet. Evol. 125, 177–187.

Kovařík, F., Fet, V., Soleglad, M.E., Yağmur, E.A., 2010. Etudes on iurids, III. Revision of the genus *Iurus* Thorell, 1876 (Scorpiones: Iuridae), with a description of two new species from Turkey. Euscorpius 95.

Krijgsman, W., Hilgen, F.J., Raffi, I., Sierro, F.J., Wilson, D.S., 1999. Chronology, causes and progression of the Messinian Salinity Crisis. Nature 400, 652–655.

Krijgsman, W., Capella, W., Simon, D., Hilgen, F.J., Kouwenhoven, T.J., Meijer, P.T., Sierro, F.J., Tulbure, M.A., van den Berg, B.C.J., van der Schee, M., Flecker, R., 2018. The Gibraltar corridor: watergate of the Messinian Salinity Crisis. Mar Geol 403, 238–246.

Kritscher, E., 1993. Ein Beitrag zur Verbreitung der Skorpione im Östlichen Mittelmeerraum. Annalen des Naturhistorischen Museums in Wien. Serie B. Botanik und Zoologie 94/95, B, 377–391.

Kuhner, M.K., 2009. Coalescent genealogy samplers: windows into population history. Trends Ecol. Evol. 24, 86–93.

Kumar, S., Stecher, G., Tamura, K., 2016. MEGA7: Molecular Evolutionary Genetics Analysis Version 7.0 for Bigger Datasets. Mol. Biol. Evol. 33, 1870–1874.

Lanfear, R., Frandsen, P.B., Wright, A.M., Senfeld, T., Calcott, B., 2016. PartitionFinder 2: new methods for selecting partitioned models of evolution for molecular andmorphological phylogenetic analyses. Mol. Biol. Evol. 34, 772–773.

Licht, A., Coster, P., Ocakoglu, F., Campbell, C., Metais, G., Mulch, A., Taylor, M., Kappelman, J., Beard, K.C., 2017. Tectono-stratigraphy of the Orhaniye Basin, Turkey: Implications for collision chronology and Paleogene biogeography of central Anatolia. J Asian Earth Sci 143, 45–58.

Lopez-Pujol, J., Lopez-Vinyallonga, S., Susanna, A., Ertugrul, K., Uysal, T., Tugay, O., Guetat, A., Garcia-Jacas, N., 2016. Speciation and genetic diversity in *Centaurea* subsect. Phalolepis in Anatolia. Sci. Rep. 6.

Loria, S.F., Prendini, L., 2020. Out of India, thrice: diversification of Asian forest scorpions reveals three colonizations of Southeast Asia. Sci Rep 10, 22301.

Matzke, N.J., 2014. Model selection in historical biogeography reveals that founder-event speciation is a crucial process in island clades. Syst. Biol. 63, 951–970.

Meijers, M.J., Brocard, G.Y., Whitney, D.L., Mulch, A., 2020. Paleoenvironmental conditions and drainage evolution of the central Anatolian lake system (Turkey) during late Miocene to Pliocene surface uplift. Geosphere 16, 490–509.

Meijers, M.J.M., Peynircioglu, A.A., Cosca, M.A., Brocard, G.Y., Whitney, D.L., Langereis, C.G., Mulch, A., 2018. Climate stability in central Anatolia during the Messinian Salinity Crisis. Palaeogeogr. Palaeoclimatol. Palaeoecol. 498, 53–67.

Minh, B.Q., Schmidt, H.A., Chernomor, O., Schrempf, D., Woodhams, M.D., von Haeseler, A., Lanfear, R., 2020. IQ-TREE 2: new models and efficient methods for phylogenetic inference in the genomic era. Mol. Biol. Evol. 37, 1530–1534.

Mutun, S., 2010. Intraspecific genetic variation and phylogeography of the oak gallwasp *Andricus caputmedusae* (Hymenoptera: Cynipidae): effects of the Anatolian Diagonal. Acta Zool. Acad. Sci. Hung. 56, 153–172.

Noroozi, J., Zare, G., Sherafati, M., Mahmoodi, M., Moser, D., Asgarpour, Z., Schneeweiss, G.M., 2019. Patterns of endemism in Turkey, the meeting point of three global biodiversity hotspots, based on three diverse families of vascular plants. Front. Ecol. Evolut. 7.

Parmakelis, A., Spanos, E., Papagiannakis, G., Louis, C., Mylonas, M., 2003. Mitochondrial DNA phylogeny and morphological diversity in the genus *Mastus* (Beck, 1837): a study in a recent (Holocene) island group (Koufonisi, south-east Crete). Biol. J. Linn. Soc. 78, 383–399.

Parmakelis, A., Pfenninger, M., Spanos, L., Papagiannakis, G., Louis, C., Mylonas, M., 2005. Inference of a radiation in *Mastus* (Gastropoda, Pulmonata, Enidae) on the island of Crete. Evolution 59, 991–1005.

Parmakelis, A., Stathi, I., Chatzaki, M., Simaiakis, S., Spanos, L., Louis, C., Mylonas, M., 2006a. Evolution of *Mesobuthus gibbosus* (Brullé, 1832) (Scorpiones: Buthidae) in the northeastern Mediterranean region. Mol. Ecol. 15, 2883–2894.

Parmakelis, A., Stathi, I., Spanos, L., Louis, C., Mylonas, M., 2006b. Phylogeography of *Iurus dufoureius* (Brullé, 1832) (Scorpiones, Iuridae). J. Biogeogr. 33, 251–260.

Parmakelis, A., Kotsakiozi, P., Stathi, I., Poulikarakou, S., Fet, V., 2013. Hidden diversity of *Euscorpius* (Scorpiones: Euscorpiidae) in Greece revealed by multilocus species-delimitation approaches. Biol. J. Linn. Soc. 110, 728–748.

Popov, S.V., Rögl, F., Rozanov, A.Y., Steininger, F.F., Shcherba, I.G., Kovac, M., 2004a. Lithological-Paleogeographic maps of Paratethy 10 maps Late Eocene to Pliocene. Schweizerbart Science Publishers, Stuttgart, Germany.

Popov, S.V., Rögl, F., Rozanov, A.Y., Steininger, F.F., Shcherba, I.G., Kovac, M., 2004b. Lithological-paleogeographic maps of Paratethys-10 maps late Eocene to pliocene.

Popov, S.V., Shcherba, I.G., Stolyarov, A.S., 2004c. Map 1: Late Eocene (PRIABONIAN - BELOGLINIAN) 37–34 Ma. In: Popov, S.V., Rögl, F., Rozanov, A.Y., Steininger, F.F., Shcherba, I.G., Kovac, M. (Eds.), Lithological-Paleogeographic Maps of Paratethys 10 Maps Late Eocene to Pliocene. Cour. Forsch.-Inst, Senckenberg, Frankfurt am Main.

Rambaut, A., Drummond, A.J., Xie, D., Baele, G., Suchard, M.A., 2018. Posterior Summarization in Bayesian Phylogenetics Using Tracer 1.7. Syst. Biol. 67, 901–904.

Ronquist, F., Teslenko, M., van der Mark, P., Ayres, D.L., Darling, A., Höhna, S., Larget, B., Liu, L., Suchard, M.A., Huelsenbeck, J.P., 2012. MrBayes 3.2: Efficient Bayesian Phylogenetic Inference and Model Choice Across a Large Model Space. Syst. Biol. 61, 539–542.

Ronquist, F., Huelsenbeck, J.P., Teslenko, M., Zhang, C.H., Nylander, J.A.A., 2020. MrBayes version 3.2 manual: tutorials and model summaries. Distributed with the software from https://github.com/NBISweden/MrBayes, pp. 1-160.

Salomone, N., Vignoli, V., Frati, F., Bernini, F., 2007. Species boundaries and phylogeography of the "*Euscorpius carpathicus* complex" (Scorpiones: Euscorpiidae) in Italy. Mol. Phylogenet. Evol. 43, 502–514.

Santibáñez-López, C.E., Aharon, S., Ballesteros, J.A., Gainett, G., Baker, C.M., González-Santillán, E., Harvey, M.S., Hassan, M.K., Abu Almaaty, A.H., Aldeyarbi, S.M., Monod, L., Ojanguren-Affilastro, A., Pinto-da-Rocha, R., Zvik, Y., Gavish-Regev, E., Sharma, P.P., 2022. Phylogenomics of scorpions reveal contemporaneous diversification of scorpion mammalian predators and mammal-active sodium channel toxins. Syst. Biol.

Santibanez-Lopez, C.E., Gonzalez-Santillan, E., Monod, L., Sharma, P.P., 2019a. Phylogenomics facilitates stable scorpion systematics: Reassessing the relationships of Vaejovidae and a new higher-level classification of Scorpiones (Arachnida). Mol. Phylogenet. Evol. 135, 22–30.

Santibanez-Lopez, C.E., Graham, M.R., Sharma, P.P., Ortiz, E., Possani, L.D., 2019b. Hadrurid scorpion toxins: evolutionary conservation and selective pressures. Toxins 11.

Santibanez-Lopez, C.E., Ojanguren-Affilastro, A.A., Sharma, P.P., 2020. Another one bites the dust: taxonomic sampling of a key genus in phylogenomic datasets reveals more non-monophyletic groups in traditional scorpion classification. Invertebr. Syst. 34, 133–143.

Scornavacca, C., Delsuc, F., Galtier, N., 2020. Phylogenetics in the Genomic Era. No commercial publisher | Authors open access book.

Şenkul, Ç., Kaya, S., 2017. Türkiye endemik bitkilerinin coğrafi dağılışı-Geographical distribution of endemic plants of Turkey. Türk Coğrafya Dergisi 69, 109–120.

Sharma, P.P., Baker, C.M., Cosgrove, J.G., Johnson, J.E., Oberski, J.T., Raven, R.J., Harvey, M.S., Boyer, S.L., Giribet, G., 2018. A revised dated phylogeny of scorpions: Phylogenomic support for ancient divergence of the temperate Gondwanan family Bothriuridae. Mol. Phylogenet. Evol. 122, 37–45.

Sharma, P.P., Fernandez, R., Esposito, L.A., Gonzalez-Santillan, E., Monod, L., 2015. Phylogenomic resolution of scorpions reveals multilevel discordance with morphological phylogenetic signal. P. Roy. Soc. B-Biol. Sci. 282.

Shorthouse, D.P., 2010. SimpleMappr, an online tool to produce publication-quality point maps.

Simon, C., Frati, F., Beckenbach, A., Crespi, B., Liu, H., Flook, P., 1994. Evolution, weighting, and phylogenetic utility of mitochondrial gene-sequences and a compilation of conserved polymerase chain-reaction primers. Ann. Entomol. Soc. Am. 87, 651–701.

Skourtanioti, E., Kapli, P., Ilgaz, Ç., Kumlutaş, Y., Avcı, A., Ahmadzadeh, F., Crnobrnja-Isailović, J., Gherghel, I., Lymberakis, P., Poulakakis, N., 2016. A reinvestigation of phylogeny and divergence times of the *Ablepharus kitaibelii* species complex (Sauria, Scincidae) based on mtDNA and nuDNA genes. Mol. Phylogenet. Evol. 103, 199–214.

Soleglad, M.E., Fet, V., 2003. High-level systematics and phylogeny of the extant scorpions (Scorpiones: Orthosterni). Euscorpius 11, 1–175.

Soleglad, M.E., Fet, V., Kovařík, F., Yağmur, E.A., 2012. Etudes on iurids, V. Further revision of *Iurus* Thorell, 1876 (Scorpiones: Iuridae), with a description of a new genus and two new species. Euscorpius 143, 1–70.

Stathi, I., Fet, V., Soleglad, M.E., 2010. Etudes on iurids, IV. Observations on *Calchas gruberi* from Megisti Island, Greece (Scorpiones: Iuridae). Euscorpius 101, 1–9.

Suchard, M.A., Lemey, P., Baele, G., Ayres, D.L., Drummond, A.J., Rambaut, A., 2018. Bayesian phylogenetic and phylodynamic data integration using BEAST 1.10. Virus Evol 4.

Vachon, M., 1971. Remarques sur le Scorpion caucasien *Calchas nordmanni* Birula (Scorpiones, Chactidae (in Russian). Entomologicheskoe Obozrenie (Revue d'Entomologie de l'URSS) 50, 712–718.

Vachon, M., 1974. Etude des caractères utilisés pour classer les familles et les genres de scorpions (Arachnides). 1. La trichobothriotaxie en arachnologie. Sigles trichobothriaux et types de trichobothriotaxie chez les scorpions 140, 859–958.

Yağmur, E.A., Soleglad, M.E., Fet, V., Kovařík, F., 2013. Etudes on iurids, VI. Further revision of *Calchas* Birula, 1899 (Scorpiones: Iuridae), with a description of a new genus and two new species. Euscorpius 159, 1–37.

Yağmur, E.A., Kovařík, F., Fet, V., Soleglad, M.E., Yeşilyurt, F., 2015a. Etudes on iurids, IX. Further analysis of a rare species *Protoiurus kadleci* (Scorpiones: Iuridae) from Turkey, based on adult males. Euscorpius 201, 1–18.

Yağmur, E.A., Soleglad, M.E., Fet, V., Kovařík, F., 2015b. Etudes on iurids, VIII. A new *Protoiurus* species from the Hidirellez Cave in Antalya, Turkey (Scorpiones: Iuridae). Euscorpius 200, 1–25.